Strain-Induced Crystallization Behavior of Natural Rubber and Trans-1,4-Polyisoprene Crosslinked Blends

Liangliang Qu, Guangsu Huang, Yijing Nie, Jinrong Wu, Gengsheng Weng, Peng Zhang

College of Polymer Science and Engineering, State Key Laboratory of Polymer Materials Engineering, Sichuan University, Chengdu 610065, China

Received 22 December 2009; accepted 12 August 2010
DOI 10.1002/app.33243
Published online 23 November 2010 in Wiley Online Library (wileyonlinelibrary.com).

ABSTRACT: The strain-induced crystallization (SIC) behaviors of crosslinked blends based on natural rubber (NR) and *trans*-1,4-polyisoprene (TPI) with different content of TPI were probed explored by using synchrotron two-dimensional wide angle X-ray diffraction and dynamic mechanical analysis. The results showed that when TPI content is less than 70% no reflection peak of TPI but NR crystallite diffractions can be observed and the diffractions of TPI βform appear when TPI content is 70 wt % in the cocured blend. SIC of cocured blends started at smaller strain ratio than the pure NR. By calculating ΔS_{def}, it is found that the drop in entropy upon strain decreased when TPI is incorporated into NR due to the reduction of molecular mobility of NR. The degree of SIC and crystallization rate index in crosslinked blends monotonously decreased with the increase of TPI content. The apparent crystallite size exhibited some surprising variations. L_{200} and L_{120} decreased with the increase of TPI content in the cocured blends. These observations were usually caused by two factors: (i) Less number of polymer chains could involve in crystal growth due to the lower mobility of polymer chains in the cocured blends which is proved by dynamic mechanical analysis results; (ii) The mean distance between nuclei decreases, which was caused by the fluctuation of crosslink density in NR phase derived from the heterogeneous distribution of curatives in two phases supported by the varying tendency of curing degree and crosslink density. © 2010 Wiley Periodicals, Inc. J Appl Polym Sci 120: 1346–1354, 2011

Key words: natural rubber; *trans*-1,4-polyisoprene; crosslinked blend; strain-induced crystallization

INTRODUCTION

Natural rubber (NR) is a kind of indispensable material for industrial application,[1,2] such as pneumatic tires for heavy-duty usages and rubber bearings for a seismic isolation system, due to its excellent tensile properties and good crack growth resistance, which derives from its prominent ability of crystallization under tensile deformation. Although NR shows lots of excellent properties, it cannot completely fulfill the industry's need for high performance materials. Recently, the commercial importance of polymer blends is increasingly attractive since the performance of individual polymer can be improved by blending. Cured blends of NR with styrene butadiene rubber (SBR),[3,4] ethylene–propylene–diene monomer (EPDM),[5,6] and *trans*-1,4-polyisoprene (TPI)[7,8] have been proved to be excellent in processibility, mechanical properties, and wear resistance. Among these, the crosslinked blend of NR and TPI has attracted much attention because it is an ideal compatible blend with good dynamic properties, such as flex fatigue resistance.[9]

To understand the enhanced properties of NR/TPI crosslinked blend, some studies on the microstructure, including the crosslink distribution[10] and crystallization behavior,[11] have been conducted. Although some interesting results have been obtained, there are still some puzzles. For examples, it is well-known that strain-induced crystallization (SIC) of NR is the origin of its excellent properties and TPI is a crystalline polymer at low crosslink density. However, what will happen when TPI and NR are cocured? Does the incorporation of TPI in NR network affect SIC of NR? And is the crystallization of TPI disordered or enhanced by NR? These questions are not clear but of utmost importance for understanding the structure–property relationship of NR/TPI crosslinked blend.

In this article, the characteristics of SIC for NR/TPI blends were explored by using the powerful synchrotron two-dimensional wide-angle X-ray diffraction (WAXD) and dynamic mechanical analysis (DMA). Some interesting new insights into the microstructure of NR/TPI blends are obtained and

Correspondence to: G. Huang (guangsu-huang@hotmail.com).

Contract grant sponsor: National Natural Sciences Foundation of China; contract grant number: 50673059.
Contract grant sponsor: National Basic Research Program (973 program); contract grant number: 2007CB714701.

TABLE I
Formulations and Network Density of the NR and Cross-Linked Blends

Sample code	0	1	2	3	4	5	6
NR(phr[a])	100	90	80	70	50	30	0
TPI	0	10	20	30	50	70	100
Stearic acid	2	2	2	2	2	2	2
ZnO	5	5	5	5	5	5	5
Antioxidant[b]	2	2	2	2	2	2	2
Accelerator CBS[c]	0.9	0.9	0.9	0.9	0.9	0.9	0.9
Sulfur	2	2	2	2	2	2	2
Curing time (min)	10	12	13	15	15	16	16
$\upsilon^{d} \times 10^{-4}$ (mol cm^{-3})	1.02	1.37	1.34	1.53	1.76	1.98	—

[a] Parts by weight per hundred parts of rubber.
[b] *N*-2-propyl-*N*′-phenyl-p-phenylenediamine.
[c] *N*-cyclohexyl-2-benzothiazole sulfonamide.
[d] Network chain density determined on the basis of classical theory of rubber elasticity.

the results will be useful for materials design of rubber products.

EXPERIMENTAL

Materials

A commercially available NR used in this study was ribbed smoked sheet (RSS) No.1 from Indonesia. TPI was provided by Qingdao University of Science and Technology (P.R.C). The synthesis technology, main structure, and properties of TPI are described in detail in Ref. 9.

Preparation of the blends

NR and TPI was used as received. The formulations for preparation of various rubber composites were shown in Table I. NR and TPI was first mixed on a two-roll mill at 75°C and then other ingredients were mixed at room temperature. The blends were crosslinked by heat-pressing at 143°C in a mold to give rubber sheets of 1 mm thickness. The ring-shaped specimens were cut from the sheets and the υ values of samples were estimated from the results of tensile measurements using the equation of the classical theory of rubber elasticity[12]:

$$\sigma = \upsilon kT(\alpha - 1/\alpha^2) \quad (1)$$

where σ is stress, k is the Boltzmann constant, T is absolute temperature, and α is stretching ratio define as $\alpha = l / l_0$, in which l_0 and l are the initial length and the length under deformation, respectively.

Measurements and characterization

The AFM analyses were performed using a SPI400 Scanning probe Microscope (Seiko Instrument Inc., Japan) under ambient conditions. In this work, analyses were always conducted in the tapping mode. The cantilever with integral silicon nitride tip was OMCL-AC200TS-C3 (spring constant: 9N/m, frequency resonance: 150 kHz, Olympus, Japan). The specimens were cooled to −100°C and surface layers were quickly sectioned off using a clean glass knife in a Leica Ultracut-R ultramicrotome. The resulting surfaces were moderately smooth (typically 500 nm peak-to-valley).

Synchrotron two-dimensional WAXD experiments were carried out under room temperature at U7B beam-line in the National Synchrotron Radiation Laboratory (NSRL), University of Science and Technology of China, Hefei, P.R.C. The wavelength used in U7B was 0.1409 nm. The two-dimensional WAXD patterns were recorded in every 180 s by Mar CCD 165 X-ray detector system. To collect WAXD patterns during deformation in real-time without holding the samples still, a homemade stretching machine with symmetric extension is used at room temperature for deformation at stretching speed of 4.2 mm/min i.e., strain rate of 0.28 min^{-1}. The original length of sample was 15 mm. The mechanical error of apparatus is less than 0.02 mm with a displacement of 100 mm. The Fit2D software package was used to analyze the 2D WAXD patterns. The software Fit2D can transform the 2D diffraction images into 1D diffraction patterns by integrating the each diffraction rings in the range of 0° to 360°. After obtaining the 1D diffraction patterns, the degree of SIC (X_c) is calculated on the basis of peak fitting during which a 2θ range from 10° to 25° was taken. X_c is defined as the ratio between the total integrated intensity of crystals (200, 201,120 reflections were taken) A_c and the total integrated intensity of crystalline and amorphous peaks A_{c+a} in the 2θ range, as expressed in the following equation:

$$X_c = \frac{A_c}{A_{c+a}} \times 100\% \quad (2)$$

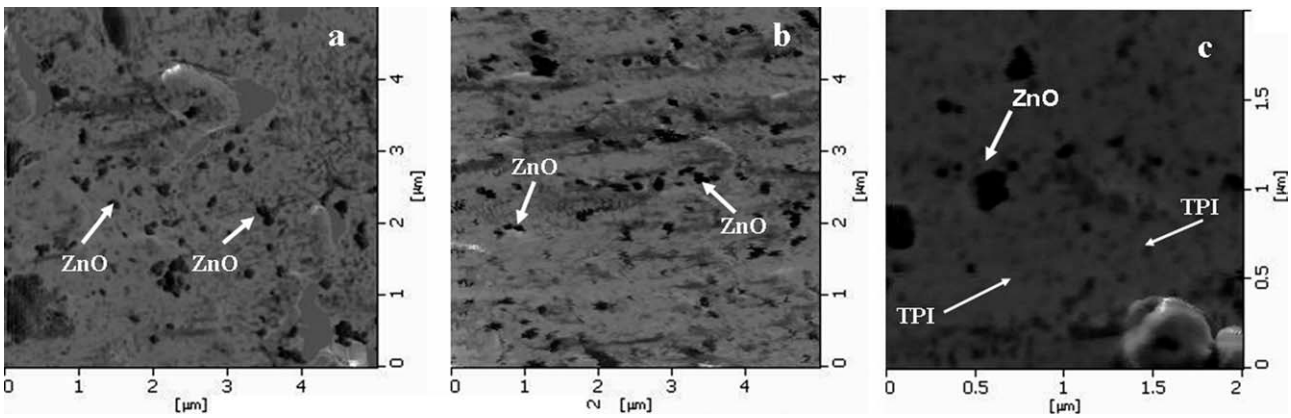

Figure 1 AFM image of NR/TPI blend, (a) large-scale(5 μm × 5 μm) image of NR/10 wt %TPI; (b) large-scale(5 μm × 5 μm) image NR/30 wt %TPI; (c) Small-scale(2 μm × 2 μm) image of NR/30 wt %TPI.

The apparent crystallite sizes were estimated by using the Scherrer equation.

$$L_{hkl} = K\lambda/(\beta \cos \theta) \quad (3)$$

where L_{hkl} is the apparent crystallite size in the direction perpendicular to the (*hkl*) plane, and β is the Bragg angle (half of the scattering angle). *K* is the Scherrer factor and value of 0.89 was used in this study.[13] β, the half-width of the *hkl* reflection in the radial direction, is determined according to Ref. 14.

DMA was studied on TA Q800 (TA instrument, USA) analyzer. The samples were trimmed to dimensions of 35 mm in length, 12 mm in wideness, and 3 mm in thickness. The dynamic mechanical properties were measured by using a dual cantilever clamp in the temperature range from −80 to 80°C at a heating rate of 3°C/min and the strain is 5%. The tests were carried out at a frequency of 1 Hz.

The tensile strength was tested on Instron 5567 material testing machine (with a 1 KN load cell) at room temperature with tensile rate of 500 mm/min according to GB/T1040-92 standard. The initial length and thickness of samples are 15 mm and 2 mm.

RESULTS AND DISCUSSION

Atomic force microscopy modulus imaging can be used to distinguish the morphology of the different phases. In Figure 1(a,b), the AFM images of NR/10%TPI and NR/30%TPI are presented. It can be observed that rubber forms soft, light, and large domains. Generally speaking, the stiffer (dark) phase is relative to higher modulus phase. To distinguish the phases the ratio of grain area obtained by SPIWin (SPI 4000 main) software (version 4.08D) can be used to determine the content ratio of dark and light domains. It can be calculated that dark domains account for about 4.21% and it is close to the mass fraction of ZnO (4.46%) in rubber blends. One can conclude that this phase is corresponding to ZnO particles. By calculating the ratio of grain area of lightly dark and light domains, it can be found that lightly dark domains account for 7.47% and 24.76% in Figure 1(a,b) respectively, which is quite equivalent to the mass fractions (8.2 wt % and 26.8 wt %) of TPI in NR/10 wt %TPI and NR/30 wt %TPI. Figure 1(c) is the magnification of NR/30%TPI sample, the dark domains (0.2–0.4 μm) is corresponding to inorganic particles. Lightly dark domains can be observed. On the other hand, Figure 1(c) reveals that TPI phase relatively homogenously disperse in NR matrix.

The dynamic mechanical spectra of samples with different content of TPI given in Figure 2(a,b) are very enlightening. The storage modulus (*E′*) curves indicate that the *E′* values of all the samples remain almost constant below glass transition temperature (T_g) and fall steeply around T_g. What should be noted in the *E′* figures is that the curve of TPI shows another sharp drop above T_g, which is attributed to the melting temperature(T_m). The temperature dependence of loss factor (tan δ) for samples is illustrated in Figure 2(b). A well-defined peak at low temperature corresponds to α-relaxation, as revealed by a strong decrease in the *E′* curves. Note that TPI displays another peak besides α-relaxation, whereas NR/TPI blends do not. This is paralleled with the results from *E′* curves. The tan δ peak relating to the α-relaxation was gradually suppressed with the increase of the content of TPI in blends. Furthermore, it is interesting to observe that in the rubbery state tan δ of the blends was obviously reduced compared with pure NR. This suggests that when TPI is blended with NR, the motion of chain segments becomes difficult. To clarify this issue, the variation of network density (υ) of NR/TPI cocured blends should be taken into account. From Table I it can be seen that when TPI is incorporated into NR, υ of blends becomes larger. That is to say, the mobility of molecular chains is lowered as υ enlarging.

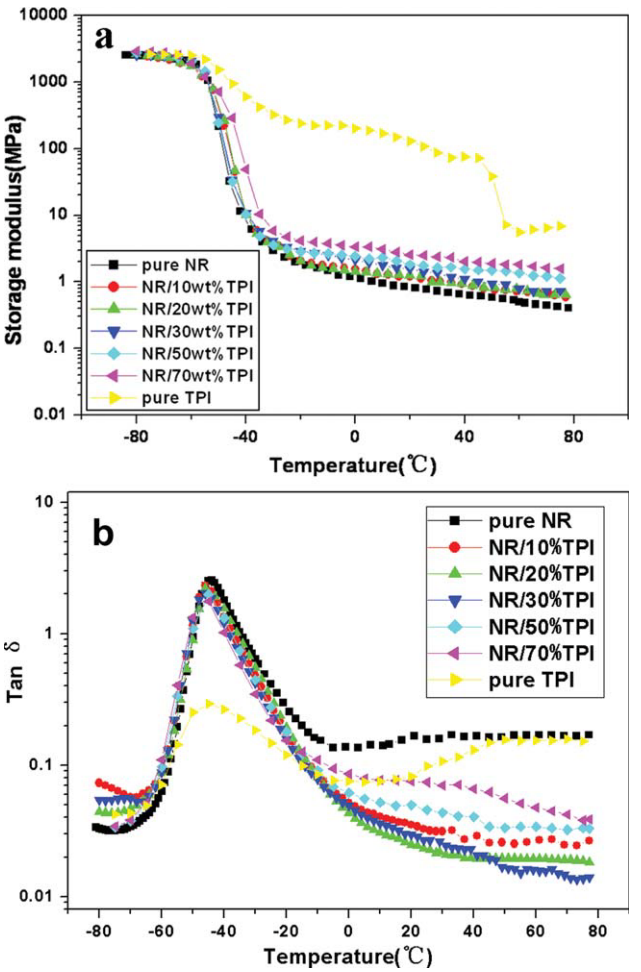

Figure 2 Variation of storage modulus (E') (a) and tan δ (b) as a function of temperature for all samples. [Color figure can be viewed in the online issue, which is available at wileyonlinelibrary.com.]

Because of the similar structure and polarity of NR and TPI, it is very difficult to characterize the covulcanization of NR/TPI blends directly. Therefore, some indirect method should be taken into account. It can been seen that in the stress-strain curves of NR and NR/TPI blends (see Fig. 3) the stress at break kept almost constant when TPI content was not over 30 wt %, whereas it reduced remarkably as the TPI amount reached 50 wt %. This is consistent with the Boochathum's report.[11] Boochathum ascribed this to the lack of the covulcanization of the two polymers due to the difference in the cure rate when large amount of TPI was blended with NR.

It has been recognized long ago that the excellent tensile property of NR originates from SIC. One wonders whether the TPI has influence on the SIC of NR. If so, is it positive or negative? These questions promote us to conduct the present study on the influence of TPI content on SIC of NR/TPI blends and in this part the blends with TPI content of 0–70 wt % was selected due to the issue mentioned in the last paragraph.

The development of crystallization behavior of all samples during tensile deformation was detected by using synchrotron WAXD. The 2D diffractions of TPI upon stretching are presented in Figure 4. It can be observed that two crystalline reflection rings at $2\theta = 18.2^\circ$ and 22° corresponding to β form crystallite appear[15] in the unstretched state and during stretching the crystallites orient along stress direction. It is noted that in the process of deformation no new reflection appears, indicating that there is no new packing structure or unit cell. The representative 2D WAXD patterns (NR/10 wt %TPI) and 1D diffraction profiles taken from 2D WAXD patterns during drawing are presented respectively, in Figure 5(a,b). For NR/10 wt %TPI cured blends, the highly oriented crystalline reflection peaks of NR (relative to 200, 201, and 120 reflections) as shown in Figure 6 start to appear at a strain around 2.7 [defined as the onset of SIC (α_c)] and the intensity of these reflections increases with strain during stretching. An interesting phenomenon must be noted is that TPI diffraction peaks can not be observed during drawing. The 2D diffraction patterns [Fig. 6(a)] and 1D diffraction profiles [Fig. 6(b)] of samples with TPI content from 0 to100 wt % at the stretched state exhibited in Figure 6. One thing should be mentioned here is that when the amount of TPI reaches 50%, the elongation of NR/TPI blends drops dramatically as shown in Figure 3. Thus, in Figure 6 the ratios selected for WAXD diffractions of sample NR/50 wt %TPI and NR/70 wt %TPI are their maximum strain ratios. It can be seen that when TPI content is less than 70%, no reflection peak of TPI but NR crystallite diffractions can be observed. A conclusion can be reached that TPI phase is free of

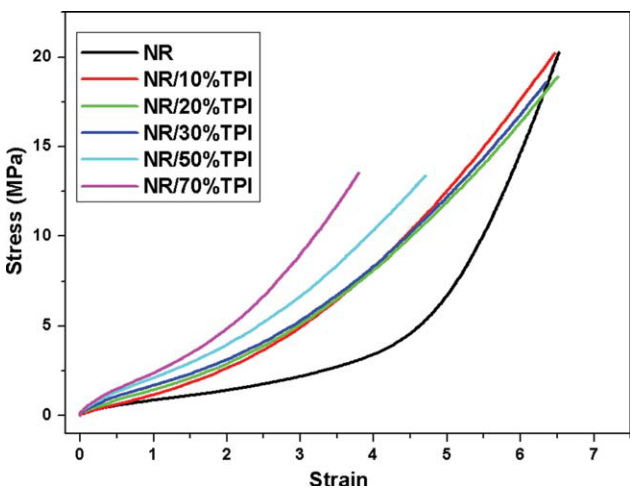

Figure 3 Stress–strain curves of NR and NR/TPI blends. [Color figure can be viewed in the online issue, which is available at wileyonlinelibrary.com.]

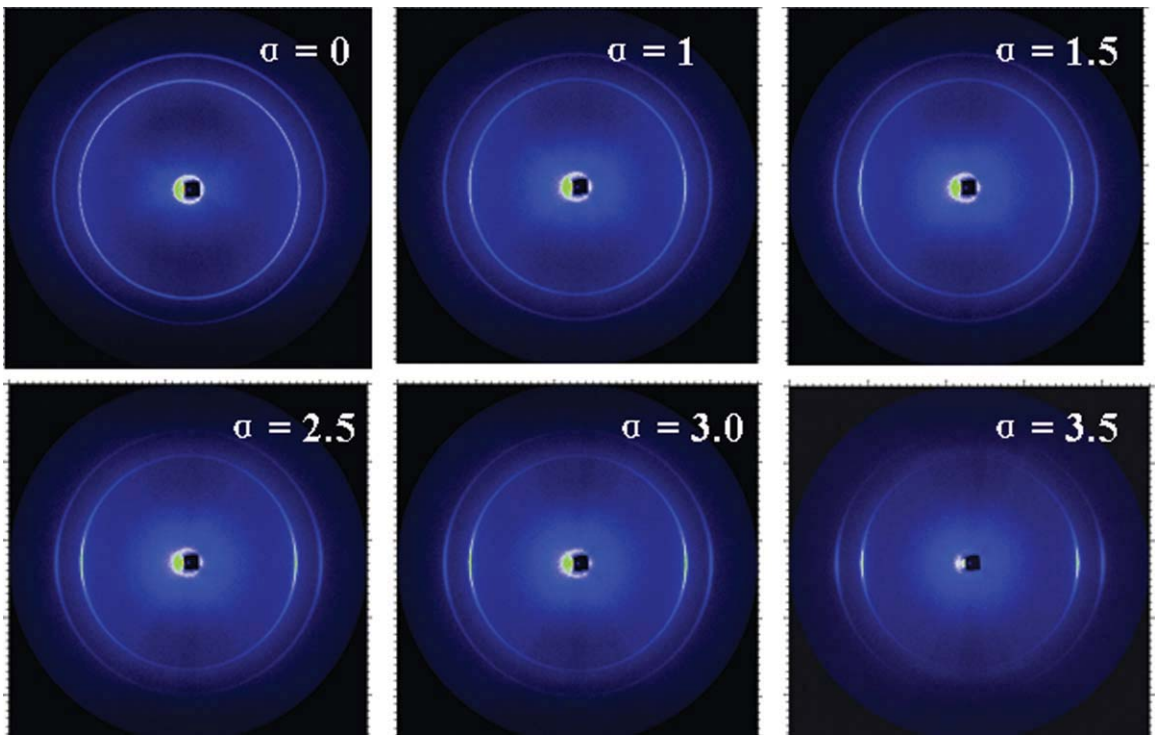

Figure 4 2D diffraction patterns of TPI. [Color figure can be viewed in the online issue, which is available at wileyonlinelibrary.com.]

crystallization when its content is not over 50 wt % in the cocured blends. This is probably ascribable to the fact that ordering of molecular chains of TPI is disrupted by NR chains in the conetworks since TPI manifests higher chain ordering than NR.[16] However, it is surprising that the diffractions of TPI βform appear when TPI content is 70 wt % in the cocured blend. To be clear, the 2D diffraction patterns of NR/70 wt %TPI are shown in Figure 7 and it is obvious that the diffraction peaks of TPI can be

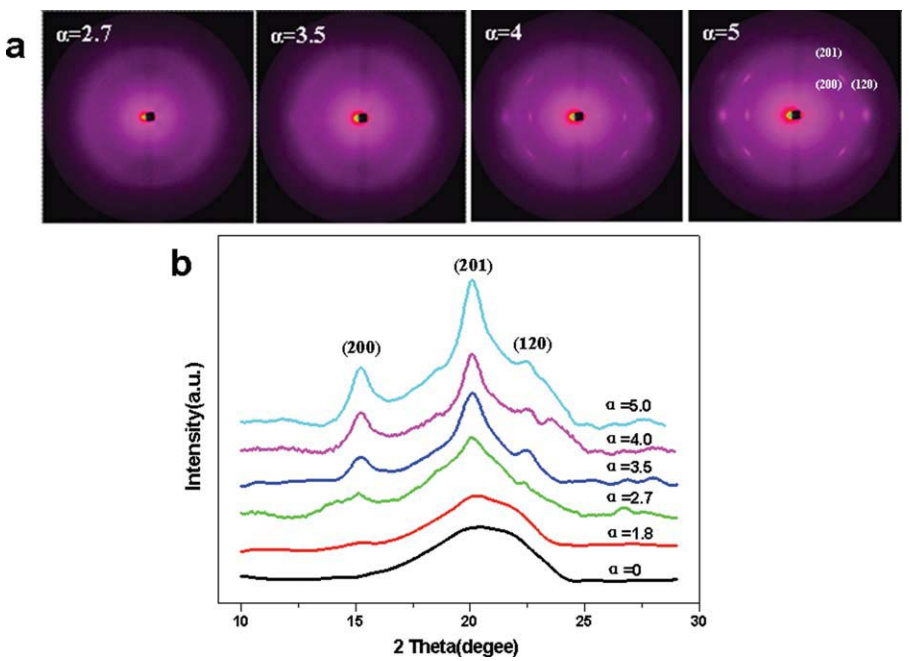

Figure 5 WAXD patterns at different strains during stretching of NR/10 wt %TPI crosslinked blend, (a) 2D diffraction patterns, (b) 1D diffraction profiles taken from 2D WAXD patterns. [Color figure can be viewed in the online issue, which is available at wileyonlinelibrary.com.]

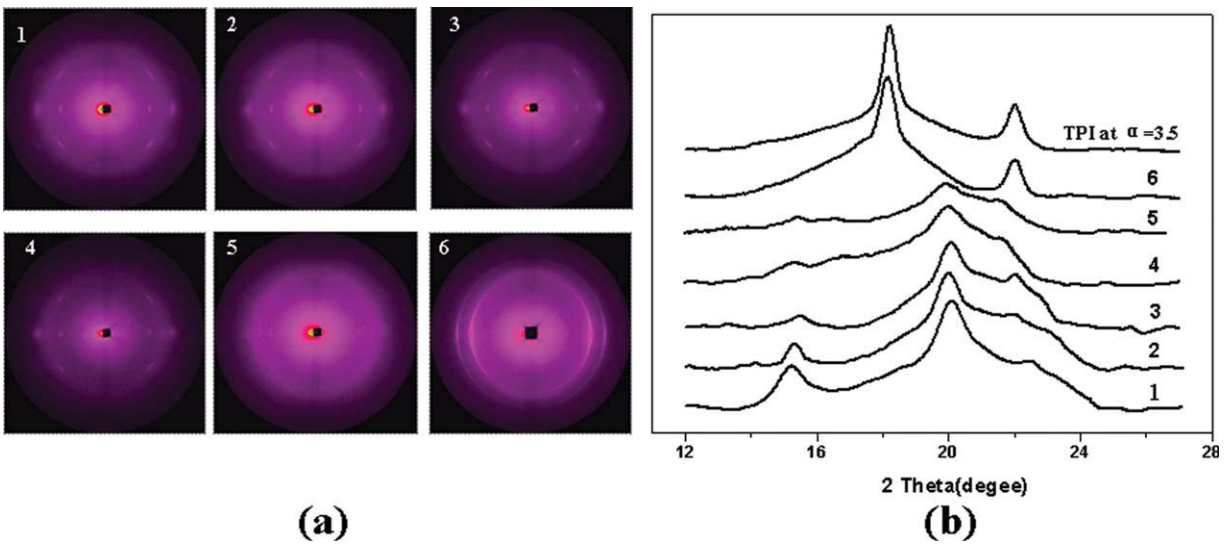

Figure 6 2D diffraction patterns (a) and 1D diffraction profiles (b) of samples with TPI content from 0 to100% at the stretched state. (1) NR at $\alpha = 5$; (2) NR/10 wt %TPI at $\alpha = 5$; (3) NR/20 wt %TPI at $\alpha = 5$; (4) NR/30 wt %TPI at $\alpha = 5$; (5) NR/50 wt %TPI at $\alpha = 4.2$; (6) NR/70wt%TPI at $\alpha = 3.3$. [Color figure can be viewed in the online issue, which is available at wileyonlinelibrary.com.]

observed in the entire process of stretching and even in the unstretched state. This can be attributed to the lack of covulcanization for the blends with higher TPI content. In that case the ordering of molecular chains in TPI phase is less disrupted in comparison to that in the blends with better covulcanization. Another thing should be noted is that NR crystallites can not be discerned in Figure 7. This is because the NR/70 wt %TPI sample breaks upon deformation before NR crystallites come into being as discussed above that the elongation of NR/70 wt %TPI sample is around 350%.

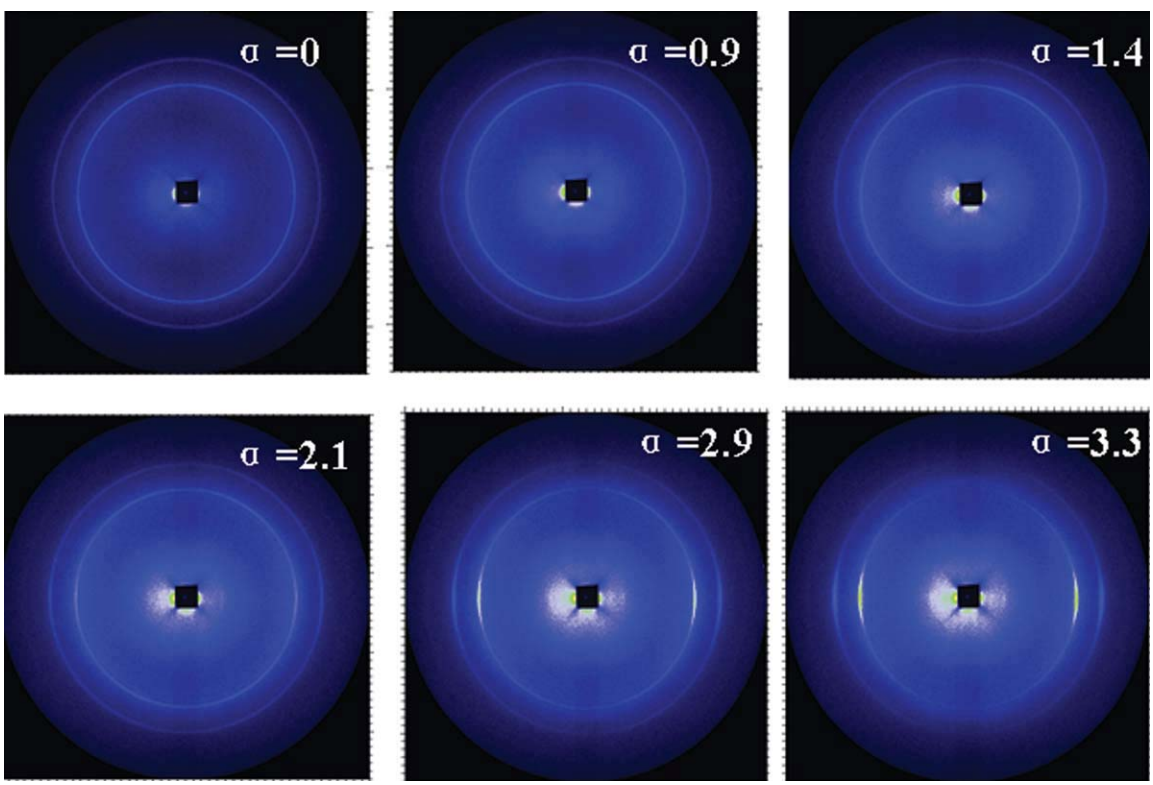

Figure 7 2D diffraction patterns of NR/70 wt %TPI at different strain ratio. [Color figure can be viewed in the online issue, which is available at wileyonlinelibrary.com.]

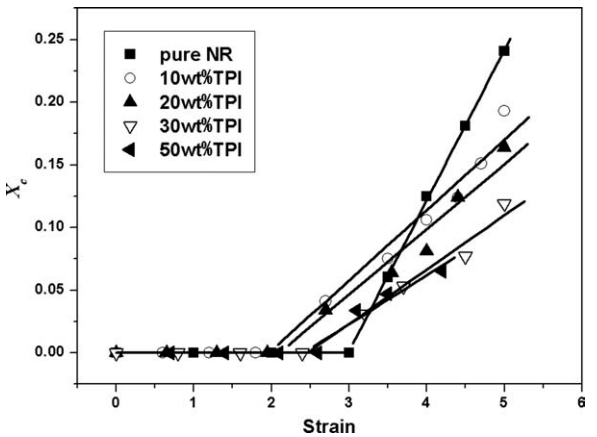

Figure 8 X_c versus strain for all samples.

To quantitatively discuss the SIC behaviors of NR/TPI blends, X_c as a function of strain and crystallization rate index (CRI) are plotted in Figures 8 and 9, respectively. From Figure 8, it is clear that all the blends exhibit smaller X_c than pure NR at large strains (exactly when strain is above 4) and X_c of blends decreases with TPI content. CRI reflects a relative SIC rate and was calculated from the slope of linearly increasing line of X_c as "CRI = (slpoe in the strain dependence of X_c)×(stain speed)."[17] It is interesting that CRI of blends exhibits dependence of TPI content in Figure 9. The reduction in mobility of polymer chain of blends, which is demonstrated by DMA and variations in network density, leads to that the diffusion and array of segment in crystalline lattice becomes difficult. On the other hand, the *trans*-structure of TPI in the blends can be considered as defects for NR chains. Increasing the amount of TPI means adding defects in the pure NR chains. These two effects produce the decreases of X_c and CRI.

Another point to be mentioned is that SIC of cocured blends starts at smaller strain ratio than the pure NR as shown in Figure 9. This interesting phenomenon has been observed in peroxide crosslinked NR,[17,18] whereas for sulfur-vulcanizated NR network it is proved that α_c remains constant regardless of υ due to its inhomogenous characteristic of the network.[17] Thus, the shift of α_c by inclusion of TPI in NR network can not be simply ascribed to the variation of υ. There must be an alternative mechanism dominating the shift of α_c.

Entropy difference between the unstretched and the stretched states(ΔS_{def}) at α_c was estimated on the base of the classical rubber elasticity theory.[19] ΔS is entropy of fusion, $\Delta S_{\text{def}} = \Delta S_\alpha - \Delta S_1$, where the subscripts α and 1 stand for the stretching ratio at deformed and undeformed states, respectively. Under the assumption of affine deformation of Gaussian chains, ΔS_{def} is represented by eq. (4)

$$\Delta S_{def} = -(1/2)\upsilon k(\alpha_1^2 + \alpha_2^2 + \alpha_3^2 - 3) \quad (4)$$

where α_1, α_2, and α_3 are stretching ratios in the direction distinguished by the subscripts. When the Poisson's ratio of the sample is 0.5, eq. (5) becomes

$$\Delta S_{def} = -(1/2)\upsilon k(\alpha^2 + 2/\alpha - 3) \quad (5)$$

ΔS_{def} at α_c of all samples was calculated and plotted versus TPI content in Figure 10. ΔS_{def} values seem to be TPI content-dependent. The drop in entropy upon strain decreased when TPI is incorporated into NR. It is indicated that for the cocured blends, the configurational entropy predrops before extension compared to pure NR. Under stretching, the entropy decreases more rapidly. Accordingly, the required reduction of entropy for the appearance of SIC can be achieved at much lower strain value. The configurational entropy of polymer chain in TPI is lower than that in NR due to the more rigid chains in TPI molecule.[20] When TPI and NR cocured, the configuration entropy of NR phase in blends is expected to be different from that in pure NR. DMA results

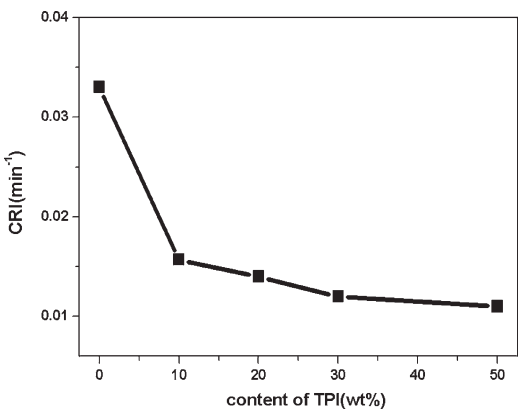

Figure 9 Effect of TPI content on CRI.

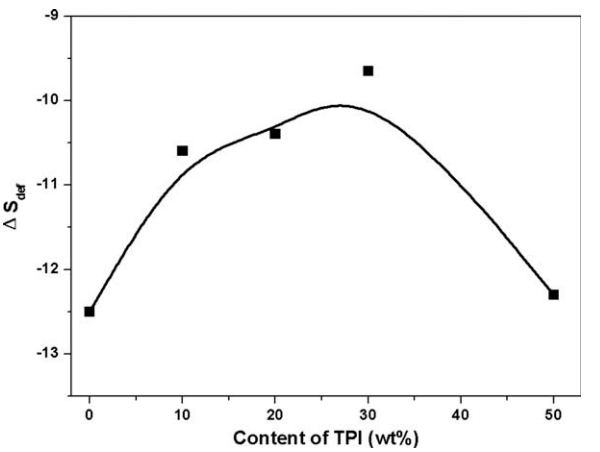

Figure 10 TPIcontent dependence of ΔS_{def} of NR/TPI blends.

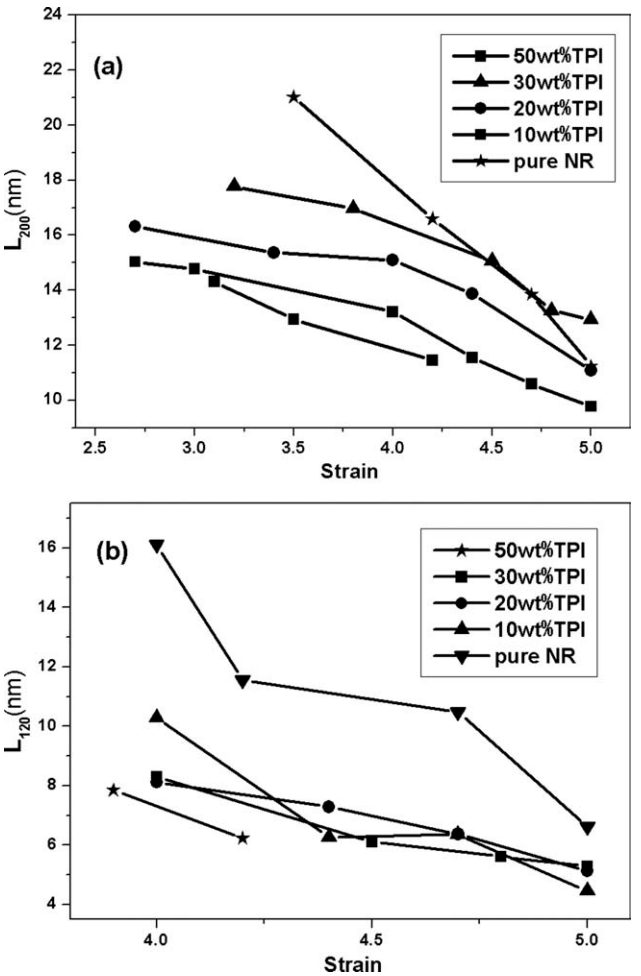

Figure 11 Strain dependence of L_{200} (a) and L_{120} (b) for NR and NR/TPI blends.

have proved that the mobility of NR molecular chains was lowered by TPI, suggesting that NR molecules in the blends were limited compared to that in pure NR and this leads to the reduction of configurational entropy of molecular chains.

To further study the influence mechanism of TPI on SIC of NR, apparent crystallite size, an important parameter to characterize the crystallization behavior of polymer, are taken into account. Figure 11 exhibits the strain dependence of apparent lateral crystallite size estimated by using 200 and 120 reflections (denoted as L_{200} and L_{120}) for all the samples. It can be observed that L_{200} value decreases with strain, which is in agreement with others' study.[14,21] It is surprising that L_{200} of the blends is smaller compared with that of pure NR and L_{200} values reduce with increasing the TPI content. These phenomena were also detected in the plot of L_{120} upon stretching. These observations are usually caused by two factors: when TPI is blended with NR, the υ increases and the motion of polymer chains are restricted, so the diffusion of polymer chains to the crystal growth front becomes difficult and less number of polymer chains can involve in crystal growth. As a result, the smaller crystallites form. On the other hand, the decrease of crystallization size is interpreted by the reduction in the mean distance between nuclei, which is due to the formation of more nuclei.[14] When two polymers are cocured, competitive vulcanization usually occurs due to the different rate of vulcanization and/or rate of diffusion of curatives including sulfur, accelerator and other compounds between the two rubber phases. Boochathum and Prajudtake[10] have clarified the different degree of vulcanization in TPI and NR phases in their crosslinked blends. In the present article, the reactivity of vulcanization reaction of NR/TPI blends was examined by comparing the height of tan δ peak for vulcanizates and nonvulcanized rubbers as shown in Figure 12. The decrease of the height of tan δ peak for vulcanizates in comparison with the nonvulcanized rubbers corresponding to

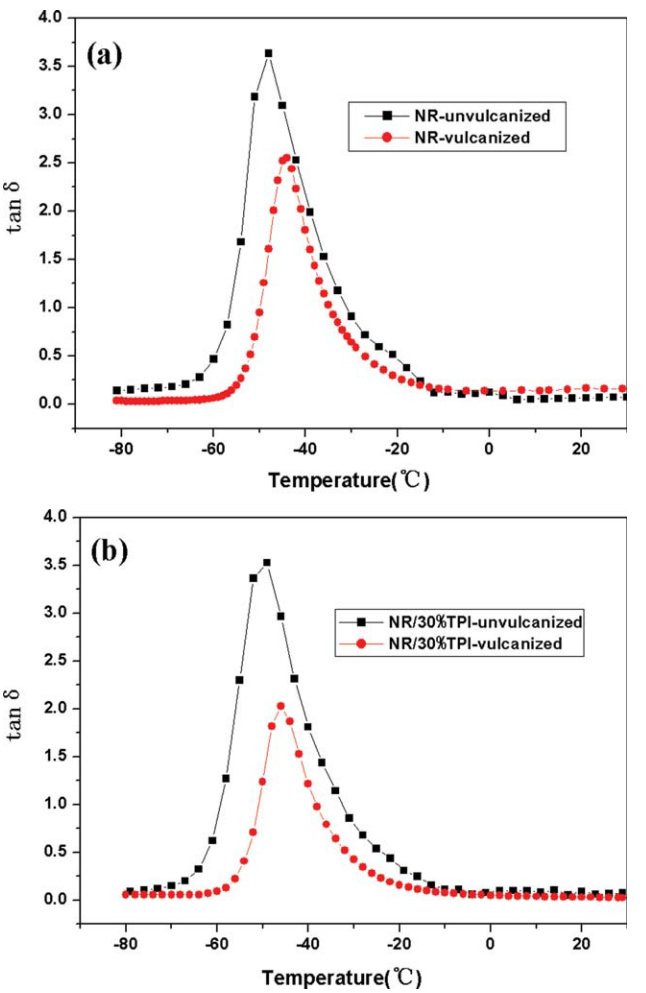

Figure 12 Tan δ curves as a function of temperature for vulcanized sample in comparison with nonvulcanized ones. (a) NR samples; (b) NR/30%TPI blend). [Color figure can be viewed in the online issue, which is available at wileyonlinelibrary.com.]

TABLE II
Decrease in the Height of Tan δ Peak for Vulcanizates Compared with the Height in Novulcanized Samples

Samples	Decrease in the height of tan δ peak (%)
NR	30.2
NR/10%TPI	38.3
NR/20%TPI	39.5
NR/30%TPI	41.7
NR/50%TPI	40.2
NR/70%TPI	29.1
TPI	17.4

the reactivity of vulcanization reaction are shown in Table II. With TPI content increases, the reactivity of vulcanization reaction tends to be greater when TPI content is not over 50%, and after that the reactivity of vulcanization reaction shows an opposite trend. This proves the conclusion made by Boochathum and Prajudtake. Hence, we have evidence to infer that when TPI is incorporated into NR, more curatives diffuse in NR phase and therefore NR undergoes higher degree of curing in comparison with pure NR at the same loading of sulfur and accelerator. The variation of the degree of curing on the TPI content is line with υ varying tendency. As a result, with the increase of TPI content in blends, υ of NR phase probably varies. The fluctuation of υ of NR phase will lead to variation in the number of nuclei in NR network. Thus, the crystallite size shows dependence of TPI content.

CONCLUSIONS

In this article, the SIC behaviors of NR/TPI blends were studied by virtue of synchrotron two-dimensional WAXD and DMA. The decrease of tan δ at glass transition and rubbery state by the incorporation of TPI suggested that the chain mobility of blends was lower in comparison to NR, which was substantiated by the difference in network densities of samples. During tensile deformation, no reflection peak of TPI but NR crystallite diffractions can be observed when TPI content is less than 70% and the diffractions of TPI βform appear when TPI content is 70 wt % in the cocured blend. α_c of cocured blends shifted to the smaller strain ratio in comparison to pure NR. By calculating $\Delta S_{def,}$ it is found that the drop in entropy upon strain decreased when TPI is incorporated into NR due to the reduction of molecular mobility of NR. X_c at large strain and CRI of NR in crosslinked blends monotonously decreased with the increase of TPI content. The apparent crystallite size exhibited some surprising variations. When TPI was incorporated in NR network, L_{200} and L_{120} decreased. These phenomena could be explained by the reduction in mobility of polymer chains. On the other hand, another reason should be taken into account was that the fluctuation of curing degree and crosslink density of NR phase derived from the heterogeneous distribution of curatives in TPI and NR phase probably produced the decrease of the mean distance between nuclei.

The authors thank Prof. Liangbin Li and Prof. Guoqiang Pan of National Synchrotron Radiation Laboratory (NSRL) in University of Science and Technology of China for their help in Synchrotron WAXD experiments.

References

1. Mark, J. E.; Erman, B.; Eirich, F. R. Eds. In Science and Technology of Rubber, 2nd ed.; Academic Press: San Diego, 1994.
2. Roberts, A. D. Ed. In Natural Rubber Science and Technology; Oxford Science Publication: Oxford, 1988.
3. Joseph, R.; George, K. E.; Joseph Francis, D. J Appl Polym Sci 1988, 35, 1818.
4. Ramesan, M. T.; Alex, R.; Khanh, N. V. React Funct Polym 2005, 62, 41.
5. Cook, S. Blends of Natural Rubber, 1st ed.; Chapman and Hall: London, 1998.
6. Sae-oui, P.; Sirisinha, C.; Thepsuwan, U.; Thapthong, P. Polym Test 2007, 26, 1062.
7. Meng, F. L.; Huang, B. C.; Yao, W.; Yu, T.; Sheng, H. B. China Synth Rubber Ind 2003, 26, 221.
8. Yao, W.; Song, J. S.; He, A. H.; Huang, B. C. Chin Elast 1995, 5, 6.
9. Song, J. S.; Huang, B. C.; Yu, D. S. J Appl Polym Sci 2001, 82, 81.
10. Boochathum, P.; Prajudtake, W. Eur Polym J 2001, 37, 417.
11. Boochathum, P.; Chiewnawin, S. Eur Polym J 2001, 37, 429.
12. Treloar L R. G. The Physics of Rubber Elasticity; Clarendon Press: Oxford, 1975.
13. Klug, H. P.; Alexander, L. E. In X-ray Diffraction Procedures for Poly-crystalline and Amorphous Materials, 2nd ed.; Wiley-Interscience: New York, 1974.
14. Tosaka, M.; Murakami, S.; Poompradub, S.; Kohjiya, S.; Ikeda, Y.; Toki, S.; Sics, I.; Hsiao, B. S. Macromoleculus 2004, 37, 3299.
15. Takahashi, Y.; Sato, T.; Tadokoro, H. J Polym Sci Polym Phys Ed 1973, 11, 233.
16. Salamone, J. C. Ed. In Polymeric Materials Encyclopedia, 1st ed.; CRC Press: Boca Raton, FL, USA, 1996; Vol. 3.
17. Ikeda, Y.; Yasuda, Y.; Hijikata, K.; Tosaka, M.; Kohjiya, S. Macromoleculus 2008, 41, 5876.
18. Ikeda, Y.; Yasuda, Y.; Makino, S.; Yamamoto, S.; Tosaka, M.; Senoo, K.; Kohjiya, S. Polymer 2007, 48, 1171.
19. Treloar, L. R. G. The Physics of Rubber Elasticity; Clarendon Press: Oxford, 1975.
20. He, M. J; Chen, X. W.; Dong, X. X. Eds. In Polymer Physics, 2nd ed.; Fudan Press: People's Republic of China, 2005.
21. Poompradub, S.; Tosaka, M.; Kohjiya, S.; Ikeda, Y.; Toki, S.; Sics, I.; Hsiao, B. S. J Appl Phys 2005, 97, 103529.